

3D Question Answering

Shuquan Ye¹ Dongdong Chen² Songfang Han³ Jing Liao^{1*}

¹ City University of Hong Kong ² Microsoft Cloud AI ³ University of California San Diego

shuquanye2-c@my.cityu.edu.hk, cddlyf@gmail.com, s5han@eng.ucsd.edu, jingliao@cityu.edu.hk

Abstract

Visual Question Answering (VQA) has witnessed tremendous progress in recent years. However, most efforts only focus on the 2D image question answering tasks. In this paper, we present the first attempt at extending VQA to the 3D domain, which can facilitate artificial intelligence’s perception of 3D real-world scenarios. Different from image based VQA, 3D Question Answering (3DQA) takes the color point cloud as input and requires both appearance and 3D geometry comprehension ability to answer the 3D-related questions. To this end, we propose a novel transformer-based 3DQA framework “3DQA-TR”, which consists of two encoders for exploiting the appearance and geometry information, respectively. The multi-modal information of appearance, geometry, and the linguistic question can finally attend to each other via a 3D-Linguistic Bert to predict the target answers. To verify the effectiveness of our proposed 3DQA framework, we further develop the first 3DQA dataset “ScanQA”, which builds on the ScanNet dataset and contains ~6K questions, ~30K answers for 806 scenes. Extensive experiments on this dataset demonstrate the obvious superiority of our proposed 3DQA framework over existing VQA frameworks, and the effectiveness of our major designs. Our code and dataset will be made publicly available to facilitate the research in this direction.

1. Introduction

In recent years, we are witnessing tremendous progress of Artificial Intelligence (AI) on vision and language understanding. Among them, Visual Question Answering (VQA) [3, 8, 21, 24, 27, 29], which finds correct answers to questions based on the understanding of images, attracts a lot of research effort. In this area, a number of datasets with well-defined tasks and evaluation protocols are introduced and various methods [3, 8, 21, 24, 27, 29] are proposed.

While existing works in VQA are primarily restricted to images, we take the first step extending it to the 3D

Question Answering (3DQA) task, i.e., answering questions given an color point cloud. A well-defined 3DQA task will broaden AI’s perception to 3D spatial understanding that mimics real-world scenarios, and benefit a wide range of applications, such as interactions of robots in real-world environments, information query in augmented reality, virtual reality, and linguistic-based navigation of autonomous vehicles. However, extending existing VQA methods to solve 3DQA is non-trivial. Unlike VQA that relies on 2D appearance information to answer questions, 3DQA has significantly higher requirement on the 3D geometry understanding. For example, to answer the first question “Is the table with the small and pink chair higher or lower than the brown desk near it?” shown in Fig. 1, it requires to understand not only the appearance, but also the geometry structure of individual objects, and even spatial relationships and spatial comparison among different objects.

To address the above challenges, we propose the first transformer based 3DQA framework “3DQA-TR”. It uses two encoders to extract geometry and appearance information from the point cloud and color point cloud, respectively. Given these appearance and geometry encodings along with question embedding, a 3D-Linguistic Bert (3D-L BERT) performs both intra-modal and inter-modal fusion to predict the target answer. Specifically, in the geometry encoder, we not only consider the geometry feature of individual objects, but also explicitly incorporate the coordinates and scales to the spatial embedding in order to model the spatial relationship between objects. And for the appearance encoder, in order to provide rich appearance information, we pretrain it on a synthetic dataset tailored for appearance information extraction.

Besides the framework, we also collect the first 3DQA dataset “ScanQA”. It builds upon the real-world indoor scene dataset ScanNet [13], which contains 1613 scans from 806 scenes. In the 3DQA dataset collection, the annotators are free to change the viewpoint and ask different types of questions, such as object appearance, object geometry, spatial relationship and their comparison. After carefully filtering and cleaning, we finally get 5,807 questions and 28,450 answers, with 4.90 answers per question on av-

*Jing Liao is the corresponding author.



Figure 1. Illustration of natural-language, free-form, open-ended questions collected for 3D scenes via Amazon Mechanical Turk. Clues for different questions are highlighted in the corresponding picture.

erage. Along with the answers, annotators’ confidence is also provided. Some example questions are shown in the Fig. 1.

To demonstrate the superiority of our framework, we compare it with representative VQA methods to answer 3DQA questions given images from ScanNet videos. The great advantage of our framework demonstrates the necessity of spatial information in the 3DQA task and the effectiveness of our method in exploiting both geometry and appearance information. Extensive ablations also demonstrate the effectiveness of our designs.

In summary, our contributions are threefold:

- **3DQA task:** We are the first to introduce the 3DQA task, which involves both language processing and 3D scene understanding.
- **3DQA-TR framework:** We design a new transformer-based framework 3DQA-TR to solve the 3DQA task. It utilizes one language tokenizer for question embedding and two encoders for extracting the appearance and geometry information, respectively, and then uses a 3D-L BERT to perform multi-modal fusion for question answering.
- **ScanQA dataset:** We build a new dataset ScanQA, which provides natural, free-form, and open-ended questions and answers in free-perspective 3D scans.

We will make our data collection tools, ScanQA dataset and code public to facilitate future research.

2. Related Work

VQA The VQA task, which combines challenges of both visual and linguistic processing to answer questions about given images, has attracted intense research efforts. Many different VQA datasets and methods have been proposed in the last few years. The most famous VQA datasets include VQA_{v1} [8] and the VQA_{v2} [21] annotated by humans, GQA [24] and CLEVR [27] with synthetic Q&As

from real-world or generated images. Based on them, several splits are further established to study bias and language prior, like the GQA-OOD [29] dataset of infrequent concepts, and the bias sensitive VQA-CP [3] dataset. As for VQA methods, advancements in deep learning have brought tremendous success in solving VQA tasks. Generally, the VQA model [6, 36, 44, 51] consists of three components - an image encoder for visual information extraction, a language encoder for question encoding, and a fusion module performing information aggregation and answer classification. Recently, Transformers [48], the de-facto standard model for language tasks, has been successfully applied to VQA as well. For example, LXMERT [46], ViLBERT [35] and VL-BERT [45], which extend the popular BERT architecture to accept joint representations of image content and natural language, have demonstrated the superiority of transformers in solving VQA tasks.

Besides standard VQA, there are some extensions of VQA to other sub-areas, such as diagrams and document analysis [9, 17, 28, 38], video understanding [20, 31, 32, 55], multiview and viewpoint selection [41], knowledge based Q&A [20, 37, 49], visual commonsense reasoning (VCR) [56], visual dialog [15] and embodied question answering (EQA) with navigation (VLN) [7, 14]. However, these extensions are still limited to 2D images and there is no extension of VQA from 2D to 3D, for answering questions about a given 3D scene. Our work takes the first step towards it and proposes a new transformer-based framework for 3D understanding and linguistic processing.

3D Vision and Language. There are also some recent works exploring 3D scene understanding through language, such as 3D object localization (e.g., [1, 10, 18, 23, 52, 54]) and 3D object captioning (e.g., [10, 12]). Among them, ScanRefer [10] is a representative work for both 3D localization and captioning, but it requires the input of multi-view photos provided by the ScanNet dataset, which greatly limits their application because 3D datasets do not always have multi-view photos along with them. In contrast, our method takes point cloud as input. Moreover, these meth-

ods and datasets for 3D localization and captioning are restricted to objects of limited categories, which is different from our free-form and open-ended question and answering task in real scenes.

In particular, MP3D-EQA [50] proposes a novel navigation task utilizing 2.5D RGB-D frames and language to navigate and answer templated questions in photorealistic environments. First, their task is different from our 3DQA. MP3D-EQA focuses on navigation, so it just supports a few object classes and only three types of template questions (location, color, color_room) which all are related to navigation. In contrast, our 3DQA questions contain a wider variety of objects, spatial and visual concepts. Moreover, their RGB-D inputs limit viewpoints in observing the 3D scene, while our point cloud input enables free views to meet the higher requirements in scene understanding brought by the free-form and open-ended questions. In addition, as their template question follows only a few forms, this task has a very limited problem diversity and low linguistic-processing difficulty. Also, the language model in their approach is not flexible - the text representation is the average of word embeddings obtained by a predefined matrix. With the above restrictions tailored for the navigation task, it is difficult to apply MP3D-EQA in our 3DQA task.

3. 3DQA Task and ScanQA Dataset

We introduce the task of 3D Question Answering with natural, free-form, and open-ended questions and answers in real-world 3D scenes. Given a 3D scene \mathcal{S} represented by point cloud of N points with color channel $\mathcal{S} \in \mathbb{R}^{N \times 6}$ ($xyzrgb$), and a question Q of T linguistic words are noted as $\{q_1, \dots, q_t, \dots, q_T\}$, the goal of 3DQA is to predict the answer \mathcal{A} .

In this section, we first present our data collection and quality control strategy. Then we analyze the question and answer statistics of the built dataset, along with the analysis of confidences and inter-subject agreements, according to which we design the evaluation metric. Based on the analysis, we also clearly show the difference between this 3DQA task and VQA.

3.1. Dataset Collection

The ScanQA dataset is built upon ScanNet [13], a real-world indoor scene dataset of 1,613 scans from 806 scenes. Different from the question and answer collection of VQA tasks, our 3D web-based UI lets the annotators freely control the viewpoint, camera setting, as well as transparency of each scan. This enables annotators to investigate various aspects of the scenes.

To ensure the *viewpoint variety* of question and answer annotations, and to encourage sufficient exploration of the scene, we reject those with overlapping camera parameters.

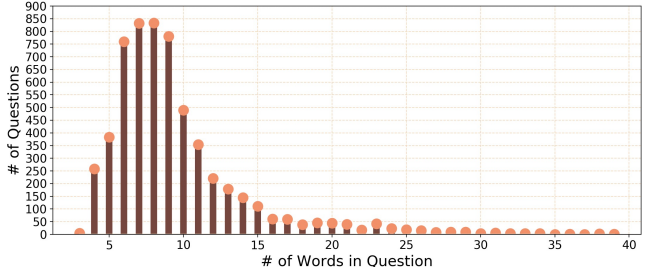


Figure 2. Question lengths distribution.

We design three methods to encourage *interesting and diverse questions*. First, we show the previously asked questions to question annotators and reject duplicated ones. Second, we utilize an online robot and encourage the annotators to stump it. Third, a rich collection of carefully selected interesting questions are shown on the instruction page as the prompt. In order to ensure the *quality* of questions and answers, besides the aforementioned online robot checker, syntax check and manual correction are also performed to reduce possible grammatical errors. All questions and answers are collected by crowdsourcing on Amazon Mechanical Turk (AMT). Along with the answers, the annotator’s confidence is also recorded.

3.2. ScanQA Dataset

In total, the ScanQA dataset provides 5,807 questions (7.2 questions per scene on average), 28,450 answers (4.9 answers per question). More details can be found in the supplementary materials.

Question and Answer Statistics. We show some typical data samples of ScanQA in Fig. 1. It shows that open-ended questions in our ScanQA dataset include a comprehensive variety of appearance and geometry concepts. For example, question 1 requires information on not only the *appearance* of a single object, but also the *geometry* of that object and a relative *spatial comparison between objects*. Question 2 captures the *placement* information from *aggregation* of more than two objects. Question 3 requires ability for *navigation to the view-point* as well as *spatial comparison to the average value*.

We analyze the question length distribution in Fig 2. It can be seen that the majority of our questions have more than 5 words, and the average length of the questions is 9.31. Please refer to the supplementary for detailed question distribution based on the first 4 words. In Fig. 3, we also provide the annotator confidence distribution over questions and analyze the relationship between confidence and inter-human labeling agreement. We observe that most questions are answered with a high level of confidence (0.8 to 1.0). From the figure, we observe that the larger the confidence, the better the agreement between different annotators. More

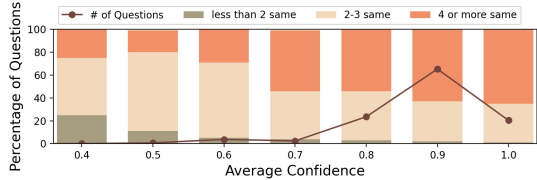


Figure 3. The line shows the question number of different confidence levels. The height of the bars represents the percentage of questions where annotators agree on the same answer, for each confidence level.

than half of questions with confidence around 0.8 receive consistent labeling from 4 or more annotators. And it is very rare that all the answers differ from each other.

Accuracy Metric. Following VQA, we define the accuracy of an answer based on the inter-human agreement. Based on observations on collected annotations, we define a question with more than 2 same labels as an accurate answer. As most answers (94.467%) are single-word, we are able to judge if two answers are consistent without additional efforts. The accuracy of an answer is defined as:

$$\text{accuracy} = \min\left(\frac{\#(\text{same annotator answer})}{2}, 1\right). \quad (1)$$

We note that although the answers are simple, it does not imply that the questions are straightforward. On the contrary, the question usually requires complex reasoning in a multi-step manner, as shown in all questions in Fig. 1.

Comparison with VQA. Compared to the previous VQA task with 2D images, our 3DQA takes a 3D scene as input and concerns more object geometry and spatial relationship between objects. We demonstrate the different characteristics between the VQA dataset and our ScanQA dataset based on question types. We first categorize questions into various types and then analyze their statistics in each dataset.

Fig. 4 illustrate the statistics of question types of our ScanQA dataset and VQA dataset. First, the spatial concept is much more important for 3D scenes, compared to perspective projected and scale agnostic images. Thus, questions about “*spatial*” concepts (e.g., scale, angle, position and their comparison), “*placement*” (e.g., symmetrical), and “*spatial comparison to average*” (e.g., to estimate a size and compare to an average one) are common in 3DQA. Second, compared to the 3D point cloud, 2D images are viewpoint specific, which arise different conventional spatial representations. For example, we commonly use words like “front”, or references like “the closer desk (to me)” to describe an object in 2D images. However, as these descriptions are viewpoint dependent, they will cause uncertainty in a 3D scene. Instead, people tend to specify

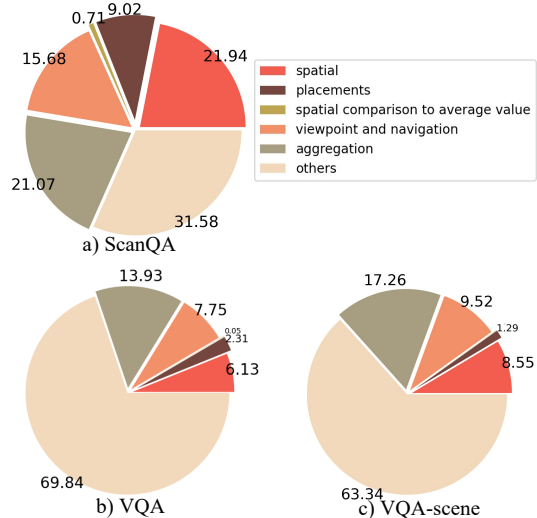


Figure 4. Question type comparison in ScanQA, VQA and VQA-scene.

one object in 3D scenes by describing a *viewpoint or doing navigation*. Third, compared to a single-view 2D image, a 3D scan reconstructed from thousands of views is less restricted by occlusion. As a result, a 3D scan generally contains much more information than one single image. In order to answer these questions specific to the 3DQA task, the network should be designed with long-term memory and information “*aggregation*” ability from more than two concerned objects.

4. Method

The overall framework of 3DQA-TR is summarized in Fig. 5. Given an input 3D scene and a corresponding question, our 3DQA-TR regresses the answer as a classification problem over all candidate answers. The candidate answers are collected from *training* split, considering both subject agreement and answer confidence.

In the geometry encoder, given a scene point cloud $\mathcal{S}' \in \mathbb{R}^{N \times 3}$ (xyz without rgb), a geometry network detects K 3D object proposals and extracts the geometry feature of each object and spatial embedding for relationship modeling. In the appearance encoder, given the point cloud $\mathcal{S} \in \mathbb{R}^{N \times 3}$ (xyz with rgb), an appearance network extracts color features for each detected object to support appearance-related questions. The extracted geometry and appearance information, as well as question embedding are further embedded as appearance, geometry and linguistic elements. Taking these elements as input, 3D-L BERT conducts both intra- and inter-modal interactions and outputs the predicted answer. Following the standard practice, our model is driven by the cross-entropy loss.

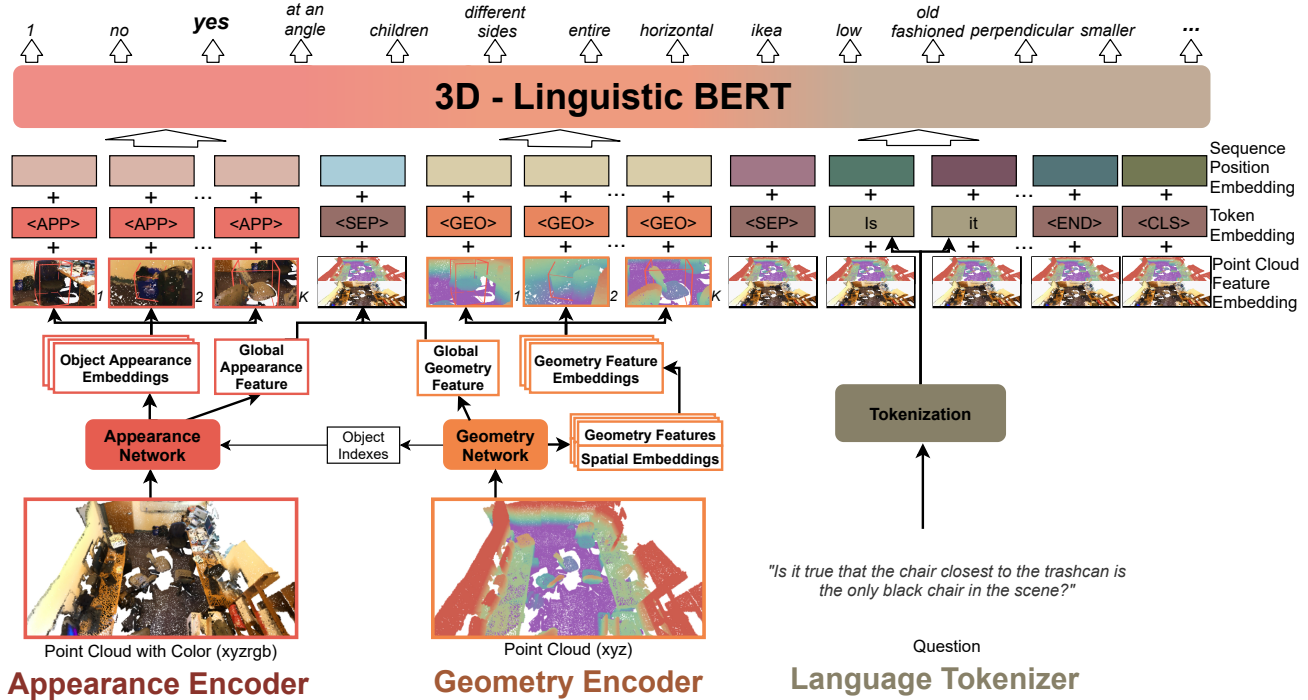


Figure 5. Illustration of our pipeline. The 3DQA-TR framework has three jointly trainable parts: appearance encoder (red), geometry encoder (orange), and 3D-L BERT. The geometry encoder provides both structure information of each object and positional and scale information to model spatial relationship between objects. The appearance encoder is used to extract appearance information. Given the encoded appearance and geometry together with question embedding, the 3D-L BERT attends to the intra- and inter- modal interactions and predicts the answer.

4.1. Geometry Encoder

We first introduce the extraction of geometry features and spatial embedding in the geometry network. Here, *Geometry features* are defined as features of each object extracted from one 3D object detection network. In details, following the common practice [33, 39, 43], we take point clouds of the entire scenes $\mathcal{S}' \in \mathbb{R}^{N \times 3}$ (xyz without rgb) as input and learn feature representations with a backbone network (PointNet++ [40] in our implementation). Then object candidates are generated by initial subsampling, and the final 3D bounding boxes of K objects are generated by 3D NMS. The object indexes of these two sampling steps are utilized to trace back to the corresponding feature representations in the backbone model and the refined representation in the detector for each object. These are served as geometry features.

Spatial embedding is to explicitly incorporate inter-object relationship to handle a number of questions about spatial relationship in 3DQA. To this end, we utilize location, scale information of each detected object. In details, we characterize each predicted bounding boxes into a 12-d vector, as $v = (\frac{x_c}{X}, \frac{y_c}{Y}, \frac{z_c}{Z}, \frac{dx}{X}, \frac{dy}{Y}, \frac{dz}{Z}, \frac{x_{min}}{X}, \frac{x_{max}}{X}, \frac{y_{min}}{Y}, \frac{y_{max}}{Y}, \frac{z_{min}}{Z}, \frac{z_{max}}{Z}) \in$

\mathbb{R}^{12} . x_c, y_c, z_c are position of the center of this box, and dx, dy, dz are scales of this box, and x_{min}, x_{max} are minimum and maximum x values of this box. To ensure the scale invariance, they are divided by the scales of this scan in X, Y, Z directions. And then a positional encoding [48] is applied to the vector.

$$\begin{cases} \text{PE}(v, 2i) = \sin(v/1000^{2i/d_{\text{model}}}) \\ \text{PE}(v, 2i+1) = \cos(v/1000^{2i/d_{\text{model}}}) \end{cases} \quad (2)$$

where $i \in [0, \dots, d_{\text{model}}/2)$ and d_{model} is the target embedding dimension. Therefore, for each object, we get a high-dimensional representation $PE(v) \in \mathbb{R}^{12 \times d_{\text{model}}}$ for the location, scale and bounds, which is regarded as the spatial embedding. Finally, we obtain K geometry features and K spatial embedding, both of which represent geometry information of K objects.

4.2. Appearance Encoder

To answer appearance-related questions, we need to extract color features for each object proposal. However, 3D object detectors tend to ignore the RGB information and mainly focus the geometry information. To mitigate this issue, we design a separate appearance encoder to capture

color information of object proposals and pre-train this appearance encoder on color-related questions.

Given a color point cloud $\mathcal{S} \in \mathbb{R}^{N \times 6}$, the appearance network outputs appearance features of each object proposal. In details, we use a PointNet++ network [40] to extract all point features, from which we select the features of each detected object by indexes and form K appearance feature. We use average-pooling to extract global appearance features from all point features.

To enforce the appearance extraction, we pre-train the appearance network on a synthetic question answering dataset tailored for appearance information extraction. This dataset consists of color-related questions generated by the template of “What color is <object>?”. Please refer to our supplement for more details. The following ablation experiments will demonstrate the effectiveness of the appearance encoder and the pretraining.

4.3. 3D-Linguistic BERT

BERT [16] model has proved its capacity to aggregate and align multi-modal information in visual-language tasks. Inspired by this, we propose one 3D-L BERT to aggregate the multi-modal information from appearance encoder, geometry encoder, and linguistic tokenizer, to make the final answer prediction. The input of 3D-L BERT is mainly composed of three types of elements: appearance, geometry, and linguistic. And some auxiliary elements for modality separation or information summarization (classification token) are also added. As shown in Fig. 5, each element is the sum of Point Cloud Feature Embedding, Token Embedding, and Sequence Position Embedding.

Point cloud feature embedding is the geometry embedding from a point cloud or appearance embedding from a color point cloud. In details, in geometry elements, they are the geometry feature embedding of K objects. To gain the geometry feature embedding, we concatenate the geometry features with spatial embedding and feed them into a fully connected layer. In appearance elements, they are appearance embedding of K objects, which are formed by feeding the appearance features into a fully connected layer. In linguistic and other auxiliary elements, they are the same embedding derived from a combination of both appearance and geometry feature of the scene. In details, it is obtained by applying a linear layer after the concatenation of global appearance and geometry features.

Token embedding in the linguistic element is the Word-Piece embedding of question following the practice in BERT. For appearance and geometry elements, a special <APP> and <GEO> token is defined. *Sequence Position embedding* is to indicate the position of an element in all elements. Specifically, positions among the appearance elements are identical since they are not sequential, and so do geometry elements.

By adaptively integrating *intra-modal* information inside each element type, 3D-L BERT enables the aggregation within geometry features or appearance features, and spatial relationship modeling among the objects represented by spatial embedding. By aligning *inter-modal* information among three different element types, the linguistic information can selectively attend to geometry or appearance clues of any object without including the redundant information. And a scaling parameter for each embedding and each element is jointly learned to achieve a good balance. The following ablation experiments about individual embedding will demonstrate the superiority of the design.

5. Experiments

We first describe the data preparation and training. Next, we show both quantitative and qualitative results of our framework compared with 2D VQA approaches, and accuracy of human participants under different input settings. We also conduct ablation experiments to demonstrate the effectiveness of our major components.

Data Preparation. We split our data into train/val/test sets following the ScanNet [13], and ensure disjoint scenes for each split. According to the type of the answers for each question, we split the test set into 4 sub-classes: Yes/No (Y/N), Color, Number, and Others. We use the accuracy defined in Eq.(1) as the evaluation metric for the following experiments.

Training. The 3D-L BERT model is initialized by the official pytorch pretrained Bert-base model as described in [16]. Before joint fine-tuning of the whole framework, the detector backbone (Group-Free [33] by default) is pre-trained on the 3D object detection task. And the appearance network is pre-trained by question answering on the synthetic color-related questions. We train our framework on train and val splits and report performances on test split.

5.1. Main Results

In Table 1, we compare our method with the representative 2D VQA method SAN [51], which takes images and questions as input. The SAN is trained with questions in ScanQA and the corresponding video frames from ScanNet as input. To favor its performance, we chose the image whose viewpoint is closest to the viewpoint of human answers for this question. In all types of questions, we find that our 3DQA-TR outperforms 2D VQA baseline. Specifically, our model improves the accuracy of spatial-related questions by around 14%. It is expected because images are insufficient to answer 3DQA questions, even for human subjects.

To show that the 3D scene comprehension is required for 3DQA, we also present a human-study experiment that examines human performance under three different input set-

	All	Number	Color	Y/N	Other	aggregation	compare-avg	placement	spatial	viewpoint
Image+Q [51]	38.00	25.08	17.85	59.91	18.51	39.97	35.00	34.74	35.45	29.39
3DQA-TR	47.88	32.50	19.64	63.69	38.48	45.20	46.88	44.49	49.11	41.54

Table 1. Comparison with VQA method SAN [51] given question and the frame with the closest view to the human answers. From left to right are overall accuracy, accuracy of different types of answers, and accuracy of different types of questions. “compare-avg” refers to spatial comparison to the average value.

Input	Human Accuracy (%)									
	All	Number	Color	Y/N	Other	aggregation	compare-avg	placement	spatial	viewpoint
Question	34.71	16.19	8.89	53.97	21.58	28.85	15.63	25.75	37.03	24.76
Question+Image	54.91	45.56	35.76	72.51	39.42	55.66	36.46	51.04	56.71	40.06
Question+Scene	73.89	82.42	47.03	89.16	56.59	76.45	75.00	71.28	77.08	70.02

Table 2. Accuracy of human answers with different input settings.

tings: 1) only the question; 2) the question and a single image that is closest to the viewpoint of human answers; 3) the question and the corresponding 3D scene. For fairness, questions are randomly chosen, and different settings of the same scene will not be assigned to the same subject. Table 2 shows that human participants who are given both question and 3D scenes perform much better than others, demonstrating the importance of 3D scene comprehension in 3DQA. Notably, the accuracy gap ($> 20.0\%$) between Question+Image and Question+Scene is bigger for spatial-related questions (rightmost five columns). On the other hand, the performance gap between human and our 3DQA-TR also shows that there is still a large room to improve.

In Fig. 6, we show some qualitative examples of 3DQA-TR, 2D VQA baseline, and human answers. In all the questions, our predictions are scored 100% correct, which demonstrates the ability of the proposed framework for both appearance and geometry comprehension.

5.2. Ablation Experiments

Component deduction. In the first three rows of Table 3, we show ablation with deducted components of our framework. In the “Qonly” row, both the appearance and geometry encoders, as well as the appearance and geometry element of the 3D-L BERT are removed. Thus it works like the original BERT model and provides a lower bound for solving 3DQA with only questions as input. It has the worst overall performance of all the baselines, indicating that information beyond question is required. We also noticed an interesting phenomenon: the accuracy is slightly higher than that of humans in the “Question” row of 2. It is not surprising because the network can learn the prior knowledge of the data distribution while the tested people are not the annotators of our dataset and have no such prior.

At the “Geo+Q” row, the appearance element is removed from the input. We can observe an overall accuracy decline compared to the full model, especially in

“Color” split, which further demonstrates the necessity of appearance information. Compared to the “Qonly” setting, obvious performance gain can be observed, especially in the “spatial”(33.95% to 48.18%), “placement”(31.69% to 41.32%), “viewpoint and do navigation”(30.64% to 40.02%) and “spatial comparison to average”(22.92% to 42.71%) subset, which we owe to the superiority of the geometry encoder. At the “App+Q” row, we removed geometry element from the input. The accuracy, especially for the “spatial”, “spatial comparison to average” and “placement” subset, drops compared with full model, indicating that the geometry information really matters. Compared to the “Qonly” setting, performance gain in the “color” (10.09% to 15.06%) split is also noticeable, demonstrating the capability of the appearance encoder.

Appearance questions pre-training. In this ablation study, we demonstrate the design of the proposed pretraining of appearance encoder in Table 3. The performance with appearance encoder trained from scratch is shown in the “AppFromScratch” row. In contrast, for our default design, the appearance encoder is pretrained on a generated question-answering dataset. On this generated dataset, our accuracy is 45.03%, which is much higher than 25.74%, the lower bound that predicts the most frequent answer to this question (e.g., “What color is the wall?”-“White”). After applying the pretraining weight and then joint-training on the ScanQA dataset, the performance is much better than the trained from scratch counterpart, especially in “color” split (improved from 12.52% to 19.64%).

Element design. We show experimental results to demonstrate that embedding geometry and appearance into one element will cause the redundancy problem. In the “OneElementForAll” row of Table 3, we embed geometry feature, spatial embedding, and appearance feature into one element by a concatenation operation, instead of embedding them into two separate elements. We can see a clear performance decline in the “OneElementForAll” setting for all

	All	Number	Color	Y/N	Other	aggregation	compare-avg	placement	spatial	viewpoint
Qonly	36.63	25.37	10.09	59.89	16.03	38.05	22.92	31.69	33.95	30.64
Geo+Q	45.69	30.61	10.39	62.80	35.86	40.65	42.71	41.32	48.18	40.02
App+Q	39.26	29.21	15.06	61.03	19.67	40.13	17.71	33.75	36.44	32.97
NoSpaEmbedding	43.48	30.05	18.67	61.27	30.23	40.22	32.29	37.83	42.24	38.16
OneElementForAll	44.48	31.41	15.84	61.06	33.38	39.60	38.54	41.02	46.93	38.97
AppFromScratch	45.79	31.43	12.52	62.54	35.77	41.02	46.88	40.14	47.56	40.81
<i>3DQA-TR</i>	47.88	32.50	19.64	63.69	38.48	45.20	46.88	44.49	49.11	41.54
<i>3DQA-TR (B)</i>	46.10	32.41	19.87	61.61	36.12	43.88	53.13	40.61	46.45	42.23

Table 3. Ablations of component deduction, spatial embedding, element design, appearance encoder pre-train and detection backbones.

VQA Baseline Image Input				
Ours Scene Input				
Question	1. Which of the two beds is larger, the blue one or the white one?	2. What is the name of the instrument in this scene?	3. Is there a poster that is not hung on the same wall with the others?	4. Is the style of the cabinet closest to the blue bed old-fashioned or modern compared to the decoration of the whole room?
Baseline Prediction	white	piano	yes	modern
Ours Prediction	equal	electric piano	yes	old-fashioned
Human Answers	equal, equal, same, they are same, equal	electric piano, keyboard, electric piano, electronic keyboard, electric piano	yes, yes, yes, yes, no	old-fashioned, old-fashioned, old, old-fashioned, modern

Figure 6. Example predictions from 2D VQA baseline and our 3DQA-TR, and human answers in ScanQA. The answers with 100% accuracy scores are in green and otherwise in red.

splits, demonstrating the necessity of our design in separating geometry and appearance elements.

Spatial embedding. Here we conduct one ablation on the geometry encoder to remove the spatial embedding with only the geometry feature left. The results are shown in the “NoSpaEmbedding” row of Table 3. The performance is worse than the full framework, especially in “placement” (44.49% to 37.83%), “spatial” (49.11% to 42.24%) and “spatial comparison to average” (46.88% to 32.29%), indicating the importance of modeling spatial information in bounding boxes and relationship among them.

Different detector. To demonstrate the generalizability of our 3DQA-TR framework, we replace the default detector Group-Free [33] with another backbone network Vote [39], denoted as 3DQA-TR(B). It also gets the comparable performance with 3DQA-TR, as shown in Table 3.

6. Conclusion

This paper presents the first attempt at extending the 2D VQA task into the 3DQA task. In order to answer questions about a real-world 3D scene, 3DQA needs to understand both appearance and 3D geometry. To this end, we propose a novel end-to-end 3DQA framework 3DQA-TR by designing a multi-modal 3D-Linguistic BERT. The appearance and geometry information are encoded by two separate encoders, and then fed into the BERT together with the question embedding to predict the final answers. To support the 3DQA task, we also develop a new dataset, “ScanQA” for this task, which contains 5,807 questions, 28,450 answers from 806 scenes. Extensive experiments and analyses have demonstrated the superiority of our 3DQA-TR over existing VQA baselines.

7. Limitations

Though we have tried our best to increase the diversity of the newly built ScanQA dataset, it is still not as diverse as existing large-scale image VQA datasets. This is mainly because ScanQA is built upon the ScanNet dataset, which only contains 806 indoor scenes. Limited diversity of the dataset will harm the generalization ability and robustness of the model. For example, our model tends to give wrong answers to the question about humans, as humans are extremely rare in this dataset. We are currently investigating large-scale 3DQA data generation to alleviate this problem.

References

- [1] Panos Achlioptas, Ahmed Abdelreheem, Fei Xia, Mohamed Elhoseiny, and Leonidas Guibas. Referit3d: Neural listeners for fine-grained 3d object identification in real-world scenes. In *European Conference on Computer Vision*, pages 422–440. Springer, 2020. 2
- [2] Aishwarya Agrawal, Dhruv Batra, and Devi Parikh. Analyzing the behavior of visual question answering models. *arXiv preprint arXiv:1606.07356*, 2016. 18
- [3] Aishwarya Agrawal, Dhruv Batra, Devi Parikh, and Anirudha Kembhavi. Don’t just assume; look and answer: Overcoming priors for visual question answering. In *Proceedings of the IEEE/CVF Conference on Computer Vision and Pattern Recognition*, pages 4971–4980, 06 2018. 1, 2
- [4] Aishwarya Agrawal, Dhruv Batra, Devi Parikh, and Anirudha Kembhavi. Don’t just assume; look and answer: Overcoming priors for visual question answering. In *Proceedings of the IEEE Conference on Computer Vision and Pattern Recognition*, pages 4971–4980, 2018. 18
- [5] Saeed Amizadeh, Hamid Palangi, Alex Polozov, Yichen Huang, and Kazuhito Koishida. Neuro-symbolic visual reasoning: Disentangling. In *International Conference on Machine Learning*, pages 279–290. PMLR, 2020. 18
- [6] Peter Anderson, Xiaodong He, Chris Buehler, Damien Teney, Mark Johnson, Stephen Gould, and Lei Zhang. Bottom-up and top-down attention for image captioning and visual question answering. In *CVPR*, 2018. 2
- [7] Peter Anderson, Qi Wu, Damien Teney, Jake Bruce, Mark Johnson, Niko Sünderhauf, Ian Reid, Stephen Gould, and Anton Van Den Hengel. Vision-and-language navigation: Interpreting visually-grounded navigation instructions in real environments. In *Proceedings of the IEEE Conference on Computer Vision and Pattern Recognition*, pages 3674–3683, 2018. 2
- [8] Stanislaw Antol, Aishwarya Agrawal, Jiasen Lu, Margaret Mitchell, Dhruv Batra, C Lawrence Zitnick, and Devi Parikh. Vqa: Visual question answering. In *Proceedings of the IEEE international conference on computer vision*, pages 2425–2433, 2015. 1, 2, 18
- [9] Ritwick Chaudhry, Sumit Shekhar, Utkarsh Gupta, Pranav Maneriker, Prann Bansal, and Ajay Joshi. Leaf-qa: Locate, encode & attend for figure question answering. *2020 IEEE Winter Conference on Applications of Computer Vision (WACV)*, pages 3501–3510, 2020. 2
- [10] Dave Zhenyu Chen, Angel X Chang, and Matthias Nießner. Scanrefer: 3d object localization in rgb-d scans using natural language. In *Computer Vision–ECCV 2020: 16th European Conference, Glasgow, UK, August 23–28, 2020, Proceedings, Part XX 16*, pages 202–221. Springer, 2020. 2, 17
- [11] Wenhui Chen, Zhe Gan, Linjie Li, Yu Cheng, William Wang, and Jingjing Liu. Meta module network for compositional visual reasoning. In *Proceedings of the IEEE/CVF Winter Conference on Applications of Computer Vision*, pages 655–664, 2021. 18
- [12] Zhenyu Chen, Ali Gholami, Matthias Niessner, and Angel X. Chang. Scan2cap: Context-aware dense captioning in rgb-d scans. In *Proceedings of the IEEE/CVF Conference on Computer Vision and Pattern Recognition (CVPR)*, pages 3193–3203, June 2021. 2
- [13] Angela Dai, Angel X. Chang, Manolis Savva, Maciej Halber, Thomas Funkhouser, and Matthias Nießner. Scannet: Richly-annotated 3d reconstructions of indoor scenes. In *Proc. Computer Vision and Pattern Recognition (CVPR), IEEE*, 2017. 1, 3, 6, 16
- [14] Abhishek Das, Samyak Datta, Georgia Gkioxari, Stefan Lee, Devi Parikh, and Dhruv Batra. Embodied question answering. In *Proceedings of the IEEE Conference on Computer Vision and Pattern Recognition*, pages 1–10, 2018. 2
- [15] Abhishek Das, Satwik Kottur, Khushi Gupta, Avi Singh, Deshraj Yadav, José MF Moura, Devi Parikh, and Dhruv Batra. Visual dialog. In *Proceedings of the IEEE Conference on Computer Vision and Pattern Recognition*, pages 326–335, 2017. 2
- [16] Jacob Devlin, Ming-Wei Chang, Kenton Lee, and Kristina Toutanova. Bert: Pre-training of deep bidirectional transformers for language understanding. *arXiv preprint arXiv:1810.04805*, 2018. 6
- [17] Samira Ebrahimi Kahou, Vincent Michalski, Adam Atkinson, Akos Kadar, Adam Trischler, and Yoshua Bengio. Figureqa: An annotated figure dataset for visual reasoning. *arXiv e-prints*, pages arXiv–1710, 2017. 2
- [18] Mingtao Feng, Zhen Li, Qi Li, Liang Zhang, XiangDong Zhang, Guangming Zhu, Hui Zhang, Yaonan Wang, and Ajmal Mian. Free-form description guided 3d visual graph network for object grounding in point cloud. *arXiv preprint arXiv:2103.16381*, 2021. 2
- [19] Haoyuan Gao, Junhua Mao, Jie Zhou, Zhiheng Huang, Lei Wang, and Wei Xu. Are you talking to a machine? dataset and methods for multilingual image question answering. *NIPS*, 2015. 18
- [20] Noa Garcia, Mayu Otani, Chenhui Chu, and Yuta Nakashima. Knowit vqa: Answering knowledge-based questions about videos. In *Proceedings of the AAAI Conference on Artificial Intelligence*, volume 34, pages 10826–10834, 2020. 2
- [21] Yash Goyal, Tejas Khot, Douglas Summers Stay, Dhruv Batra, and Devi Parikh. Making the v in vqa matter: Elevating the role of image understanding in visual question answering. In *Proceedings of the IEEE/CVF Conference on Computer Vision and Pattern Recognition*, pages 6325–6334, 07 2017. 1, 2

- [22] Yash Goyal, Tejas Khot, Douglas Summers-Stay, Dhruv Batra, and Devi Parikh. Making the v in vqa matter: Elevating the role of image understanding in visual question answering. In *Proceedings of the IEEE Conference on Computer Vision and Pattern Recognition*, pages 6904–6913, 2017. 18
- [23] Pin-Hao Huang, Han-Hung Lee, Hwann-Tzong Chen, and Tyng-Luh Liu. Text-guided graph neural networks for referring 3d instance segmentation. In *Proceedings of the AAAI Conference on Artificial Intelligence*, volume 35, pages 1610–1618, 2021. 2
- [24] Drew Hudson and Christopher Manning. Gqa: A new dataset for real-world visual reasoning and compositional question answering. In *Proceedings of the IEEE/CVF Conference on Computer Vision and Pattern Recognition*, pages 6693–6702, 06 2019. 1, 2
- [25] Drew A Hudson and Christopher D Manning. Gqa: A new dataset for real-world visual reasoning and compositional question answering. In *Proceedings of the IEEE/CVF conference on computer vision and pattern recognition*, pages 6700–6709, 2019. 18
- [26] Justin Johnson, Bharath Hariharan, Laurens Van Der Maaten, Li Fei-Fei, C Lawrence Zitnick, and Ross Girshick. Clevr: A diagnostic dataset for compositional language and elementary visual reasoning. In *Proceedings of the IEEE conference on computer vision and pattern recognition*, pages 2901–2910, 2017. 18
- [27] Justin Johnson, Bharath Hariharan, Laurens van der Maaten, Li Fei-Fei, C. Zitnick, and Ross Girshick. Clevr: A diagnostic dataset for compositional language and elementary visual reasoning. In *Proceedings of the IEEE/CVF Conference on Computer Vision and Pattern Recognition*, pages 1988–1997, 07 2017. 1, 2
- [28] Kushal Kafle, Brian Price, Scott Cohen, and Christopher Kanan. Dvqa: Understanding data visualizations via question answering. In *Proceedings of the IEEE conference on computer vision and pattern recognition*, pages 5648–5656, 2018. 2
- [29] Corentin Kervadec, Grigory Antipov, Moez Baccouche, and Christian Wolf. Roses are red, violets are blue... but should vqa expect them to? In *Proceedings of the IEEE/CVF Conference on Computer Vision and Pattern Recognition*, pages 1, 2, 3, 4, 7, 8, 2021. 1, 2
- [30] Ranjay Krishna, Yuke Zhu, Oliver Groth, Justin Johnson, Kenji Hata, Joshua Kravitz, Stephanie Chen, Yannis Kalantidis, Li-Jia Li, David A Shamma, et al. Visual genome: Connecting language and vision using crowdsourced dense image annotations. *International journal of computer vision*, 123(1):32–73, 2017. 18
- [31] Jie Lei, Licheng Yu, Mohit Bansal, and Tamara L Berg. Tvqa: Localized, compositional video question answering. In *EMNLP*, 2018. 2
- [32] Jie Lei, Licheng Yu, Tamara L Berg, and Mohit Bansal. Tvqa+: Spatio-temporal grounding for video question answering. In *Tech Report, arXiv*, 2019. 2
- [33] Ze Liu, Zheng Zhang, Yue Cao, Han Hu, and Xin Tong. Group-free 3d object detection via transformers. *arXiv preprint arXiv:2104.00678*, 2021. 5, 6, 8
- [34] Ilya Loshchilov and Frank Hutter. Decoupled weight decay regularization. In *International Conference on Learning Representations*, 2018. 17
- [35] Jiasen Lu, Dhruv Batra, Devi Parikh, and Stefan Lee. VILBERT: Pretraining task-agnostic visiolinguistic representations for vision-and-language tasks. In *Advances in Neural Information Processing Systems*, pages 13–23, 2019. 2
- [36] Jiasen Lu, Jianwei Yang, Dhruv Batra, and Devi Parikh. Hierarchical question-image co-attention for visual question answering. *Advances in neural information processing systems*, 29:289–297, 2016. 2
- [37] Kenneth Marino, Mohammad Rastegari, Ali Farhadi, and Roozbeh Mottaghi. Ok-vqa: A visual question answering benchmark requiring external knowledge. In *Proceedings of the IEEE/CVF Conference on Computer Vision and Pattern Recognition*, pages 3195–3204, 2019. 2
- [38] Minesh Mathew, Dimosthenis Karatzas, and CV Jawahar. Docvqa: A dataset for vqa on document images. In *Proceedings of the IEEE/CVF Winter Conference on Applications of Computer Vision*, pages 2200–2209, 2021. 2
- [39] Charles R Qi, Or Litany, Kaiming He, and Leonidas J Guibas. Deep hough voting for 3d object detection in point clouds. In *Proceedings of the IEEE International Conference on Computer Vision*, 2019. 5, 8
- [40] Charles Ruizhongtai Qi, Li Yi, Hao Su, and Leonidas J Guibas. Pointnet++: Deep hierarchical feature learning on point sets in a metric space. *Advances in Neural Information Processing Systems*, 30, 2017. 5, 6
- [41] Yue Qiu, Yutaka Satoh, Ryota Suzuki, Kenji Iwata, and Hirokatsu Kataoka. Multi-view visual question answering with active viewpoint selection. *Sensors*, 20(8), 2020. 2
- [42] Mengye Ren, Ryan Kiros, and Richard Zemel. Exploring models and data for image question answering. *Advances in neural information processing systems*, 28:2953–2961, 2015. 18
- [43] Shaoshuai Shi, Xiaogang Wang, and Hongsheng Li. Pointcnn: 3d object proposal generation and detection from point cloud. In *The IEEE Conference on Computer Vision and Pattern Recognition (CVPR)*, June 2019. 5
- [44] Amanpreet Singh, Vivek Natarajan, Yu Jiang, Xinlei Chen, Meet Shah, Marcus Rohrbach, Dhruv Batra, and Devi Parikh. Pythia-a platform for vision & language research. In *SysML Workshop, NeurIPS*, volume 2018, 2018. 2
- [45] Weijie Su, Xizhou Zhu, Yue Cao, Bin Li, Lewei Lu, Furu Wei, and Jifeng Dai. VI-BERT: Pre-training of generic visiolinguistic representations. In *International Conference on Learning Representations*, 2020. 2
- [46] Hao Tan and Mohit Bansal. Lxmert: Learning cross-modality encoder representations from transformers. In *Proceedings of the 2019 Conference on Empirical Methods in Natural Language Processing*, 2019. 2
- [47] Makarand Tapaswi, Yukun Zhu, Rainer Stiefel, Antonio Torralba, Raquel Urtasun, and Sanja Fidler. Movieqa: Understanding stories in movies through question-answering. In *Proceedings of the IEEE conference on computer vision and pattern recognition*, pages 4631–4640, 2016. 18

- [48] Ashish Vaswani, Noam Shazeer, Niki Parmar, Jakob Uszkoreit, Llion Jones, Aidan N Gomez, Łukasz Kaiser, and Illia Polosukhin. Attention is all you need. In *Advances in neural information processing systems*, pages 5998–6008, 2017. [2](#), [5](#)
- [49] Peng Wang, Qi Wu, Chunhua Shen, Anthony Dick, and Anton Van Den Hengel. Fvqa: Fact-based visual question answering. *IEEE transactions on pattern analysis and machine intelligence*, 40(10):2413–2427, 2017. [2](#)
- [50] Erik Wijmans, Samyak Datta, Oleksandr Maksymets, Abhishek Das, Georgia Gkioxari, Stefan Lee, Irfan Essa, Devi Parikh, and Dhruv Batra. Embodied question answering in photorealistic environments with point cloud perception. In *Proceedings of the IEEE/CVF Conference on Computer Vision and Pattern Recognition*, pages 6659–6668, 2019. [3](#)
- [51] Zichao Yang, Xiaodong He, Jianfeng Gao, Li Deng, and Alex Smola. Stacked attention networks for image question answering. In *Proceedings of the IEEE conference on computer vision and pattern recognition*, pages 21–29, 2016. [2](#), [6](#), [7](#)
- [52] Zhengyuan Yang, Songyang Zhang, Liwei Wang, and Jiebo Luo. Sat: 2d semantics assisted training for 3d visual grounding. *ICCV*, 2021. [2](#)
- [53] Licheng Yu, Eunbyung Park, Alexander C Berg, and Tamara L Berg. Visual madlibs: Fill in the blank image generation and question answering. *arXiv preprint arXiv:1506.00278*, 2015. [18](#)
- [54] Zhihao Yuan, Xu Yan, Yinghong Liao, Ruimao Zhang, Sheng Wang, Zhen Li, and Shuguang Cui. Instancerefer: Cooperative holistic understanding for visual grounding on point clouds through instance multi-level contextual referring. In *Proceedings of the IEEE/CVF International Conference on Computer Vision*, pages 1791–1800, 2021. [2](#)
- [55] Amir Zadeh, Michael Chan, Paul Pu Liang, Edmund Tong, and Louis-Philippe Morency. Social-iq: A question answering benchmark for artificial social intelligence. In *Proceedings of the IEEE/CVF Conference on Computer Vision and Pattern Recognition*, pages 8807–8817, 2019. [2](#)
- [56] Rowan Zellers, Yonatan Bisk, Ali Farhadi, and Yejin Choi. From recognition to cognition: Visual commonsense reasoning. In *Proceedings of the IEEE/CVF Conference on Computer Vision and Pattern Recognition*, pages 6720–6731, 2019. [2](#)
- [57] Peng Zhang, Yash Goyal, Douglas Summers-Stay, Dhruv Batra, and Devi Parikh. Yin and yang: Balancing and answering binary visual questions. In *Proceedings of the IEEE Conference on Computer Vision and Pattern Recognition*, pages 5014–5022, 2016. [18](#)
- [58] Yuke Zhu, Oliver Groth, Michael Bernstein, and Li Fei-Fei. Visual7w: Grounded question answering in images. In *Proceedings of the IEEE conference on computer vision and pattern recognition*, pages 4995–5004, 2016. [18](#)

8. More Qualitative Examples

In addition to Fig. 6 in our main paper, we show more qualitative results of our 3DQA Transformer (3DQA-TR) framework in the proposed ScanQA dataset in Fig. 7. In comparison with the 2D VQA baseline, ours prediction gains higher scores.

9. Collection Details and Additional Analysis on ScanQA Dataset

9.1. ScanQA Dataset Collection

Data collection pipeline. To collect the ScanQA dataset, we have two tasks. In Task1, we collect the annotator’s questions together with his or her answers. Then in the Task2, we collect more answers from other annotators to each question collected in task1.

Web-based annotation website. Fig. 8 (left) shows the instruction page of our web-based UI for annotation pipelines of Task1 and Task2, as well as basic operations. The right image shows several samples to the annotator, which includes some selected interesting questions for different scenes in order to encourage *interesting and diverse questions*.

Fig. 9 illustrates the detailed instruction page and annotation page for Task1. As shown in the instruction page (the left image), in order to ensure the *quality and diversity* of questions, we claim that annotators need to stump a smart robot. Actually, we defined an online robot checker. It will reject easy-to-answer questions about the existence, counts, or colors of predefined known object classes, and also questions about known scene types, as well as questions that are too simple. These predefined known objects (e.g., wall, floor, cabinet) and scene classes (e.g., bedroom, hotel, living room) are shown on this instruction page. In detail, we defined different patterns for easy-to-answer questions and rejected questions that fit into these patterns:

- Existence Pattern: Is|Are there a|an|any|some <KnownObjectClass> ...? (with < 8 words)
- Count Pattern: How many <KnownObjectClass> [is|are|in in|there|this|the] ...? (with < 9 words)
- Color Pattern: What color|colour is|are the <KnownObjectClass> [is|are|in in|there|this|the] ...? (with < 6 words)
- Scene Type Pattern: Is it|this [scene|scan|room] a|an <KnownSceneClass> ...?

To further encourage *interesting and diverse questions*, we show the previously asked questions to the annotators and reject duplicates, as illustrated in Fig. 8 (right). In addition, we encourage annotators to ask questions specific to

the scene rather than generic questions. Unlike in VQA, the UI for both question and answer annotation shows the scans in the form of colored meshes, allowing annotators to freely control the viewpoint and camera settings via rotation, move, and zoom operations, as well as the transparency of mesh surfaces. Annotators are also free to explore different scans of the same scene in order to better understand the scenario. To *speed up* annotation, the page will automatically jump to the next question or scene after submission.

The instruction page and annotation page for Task2 is illustrated in Fig. 10. Like in VQA, human subjects are asked to provide ‘brief phrase’ answers instead of sentences. Answer annotators are required to answer the given question according to the corresponding scene. Along with the answers, the confidence by each annotator of his answer is collected by clicking ‘yes’, ‘maybe’, and ‘no’ before submission, which is used to generate candidate answer vocabulary. Annotators can freely control the viewpoint and camera settings from PC devices by rotating, moving, and zooming. For annotators using mobile devices, six green buttons (‘UP’, ‘Dn’, ...) have been added to the right side of this page for more convenient viewpoint control. We collected the viewpoints and camera parameters of each submitted answer and rejected the duplicate viewpoints to encourage the annotators to investigate *various aspects* of the scenes.

9.2. ScanQA Dataset Analysis

9.2.1 Question Distribution Based on First Four Words.

In Fig. 11, we show the distribution of questions, roughly grouped by their first four words. Besides questions that require appearance information (e.g., questions begin with ‘is the color of’, ‘is there natural light’), there are several types of questions that capture spatial concepts (e.g., ‘is this room spacious’, ‘is this a narrow/large/small’, ‘is this a large/’, ‘what is on/hanging/next’, ‘what shape’, ‘can you reach’) and placement (e.g., ‘is the arrangement’). Also, a certain percentage of the questions shown here necessitate navigation ability (e.g., ‘stand/sit/standing/sitting’) as well as the ability to aggregate from more than two objects (e.g., ‘is/are there any’, ‘how many different’, ‘are all’, ‘which is closer to’).

9.2.2 Answer Distributions over Different Type of Questions

The distribution of answers across different types of questions, grouped by their first words, is depicted in Fig. 12. The top answers or other answers for each question type are in different colors, and the heights of the bars indicate the occurrence numbers. It can be observed that only a few

VQA Baseline Image Input				
Ours Scene Input				
Question	1. Standing in the middle of the room facing the bookshelf, is the calligraphy work on the left or the right?	2. What instrument is covered by the silver and white cloth?	3. Standing in the middle of the room facing the curtain, is the window and the displaying monitor on the same side or different sides of you?	4. Is this a rectangular room?
Baseline Prediction	right	electric piano	no	yes
Ours Prediction	left	electric piano	yes	no
Human Answers	left, left, right, left	electric piano, keyboard, electric piano, electronic keyboard, electronic organ	yes, yes, yes, yes, yes	no, no, no, no

VQA Baseline Image Input				
Ours Scene Input				
Question	1. Is the dining table the tallest table in the room?	2. What is the material of the vintage cabinet's transparent upper part, which is next to the dining table?	3. When you walk into the room from the balcony, where is the dining table?	4. Is the cabinet with a basket on it to your left or right as you sit on the sofa with a lamp next to it and face the TV?
Baseline Prediction	yes	wood	right	right
Ours Prediction	yes	glass	right	right
Human Answers	yes, yes, yes, yes	glass, glass, mirror, glass	right, right front, right, in the front	left, left, left, left

Figure 7. Example predictions from 2D VQA baseline and our 3DQA-TR, and human answers in ScanQA. The answers with 100% accuracy scores are in green and otherwise in red.

The screenshot shows the AMT interface for the 3DQA-TR task. It includes a 'Task1 Annotation Process' section with instructions on how to answer questions, a 'Task2 Annotation Process' section, and a list of 'Some Example Questions' with corresponding images and multiple-choice options. The questions are similar to those shown in Figure 7.

Figure 8. Our instruction page for the Amazon Mechanical Turk (AMT) interface, which shows the annotation pipeline and interesting questions as prompts.

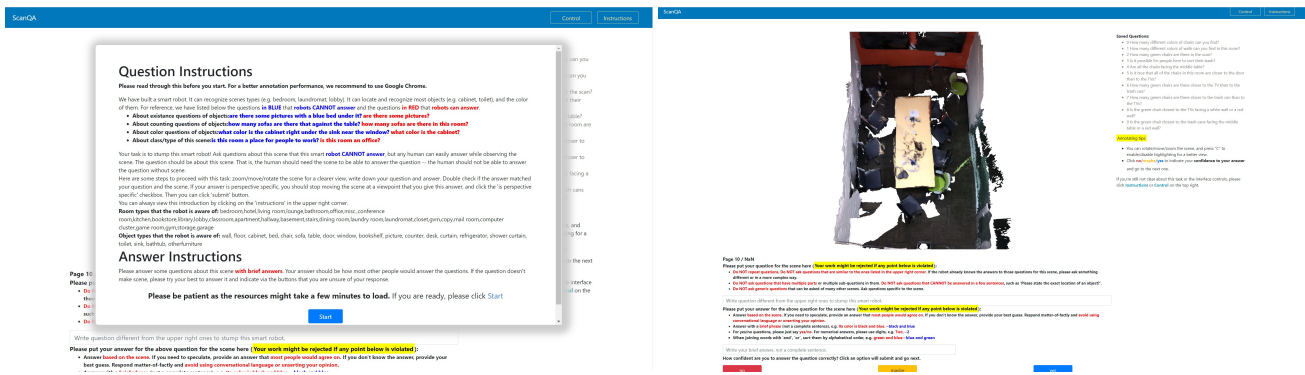


Figure 9. Our instruction page and annotation page for Task1 in AMT interface.

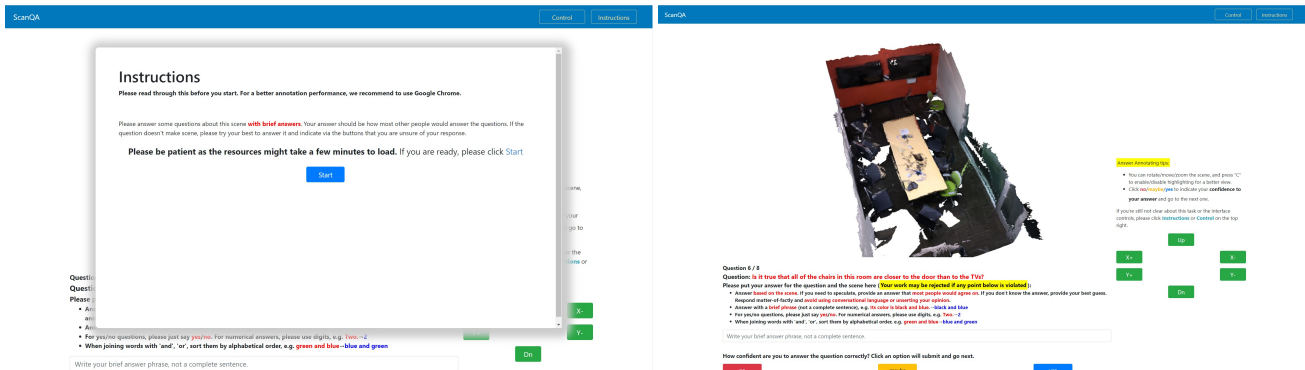


Figure 10. Our instruction page and annotation page for Task2 in AMT interface.

types of questions can be generally answered by ‘yes’ or ‘no’ (e.g., ‘can people’, ‘can you’, ‘is there’), whereas the answers to the majority of question types have rich diversity.

9.2.3 Comparison with VQA

Question type classification. The comparison between ScanQA, VQA and VQA-scene given by Fig. 4 in our main paper classifies the questions based on appearances of different types of words in each question. In detail, each question is classified into at most one class among ‘spatial’, ‘spatial comparison to the average value’, ‘placement’, ‘viewpoint and do navigation’, and ‘aggregation’:

- For ‘spatial’ type of question, it is the question with words ‘big’, ‘small’, ‘great’, ‘tall’, ‘short’, ‘high’, ‘low’, ‘size’, ‘height’, ‘length’, ‘width’, ‘angle’, ‘parallel’, ‘wide’, ‘vertical’, ‘opposite’, ‘tilt’, ‘diagonal’, ‘near’, ‘by’, ‘between’, ‘long’, ‘shape’, ‘next’, ‘fit’, ‘far’, ‘close’, ‘space’, ‘cluttered’, ‘narrow’, ‘spacious’, ‘bigger’, ‘greater’, ‘smaller’, ‘taller’, ‘shorter’, ‘higher’, ‘lower’, ‘longer’, ‘closer’, ‘farther’, ‘inside’.
- For ‘spatial comparison to the average value’ type of question, it is the question with words ‘average’, ‘large

scene’, ‘small scene’, ‘large sized’, ‘small sized’, ‘high ceiling’.

- For ‘placement’ type of question, it is the question with words ‘placed’, ‘arrange’, ‘neat’, ‘perpendicular’, ‘straight’, ‘form’, ‘symmetrical’, ‘covered’, ‘put’, ‘horizontal’, ‘surrounded’, ‘row’, ‘line’, ‘separate’, ‘partition’, ‘sloped’.
- For ‘viewpoint and do navigation’ type of question, it is the question with words ‘stand’, ‘sit’, ‘walk’, ‘go’, ‘into’, ‘face’, ‘facing’, ‘look’, ‘see’, ‘your’, ‘against’, ‘above’, ‘middle’, ‘side’.
- For ‘aggregation’ type of question, it is the question with words ‘many’, ‘all’, ‘any’, ‘largest’, ‘farthest’, ‘most’, ‘least’, ‘nearest’, ‘total’, ‘nothing’, ‘highest’, ‘brightest’, ‘else’, ‘special’, ‘every’, ‘entire’, ‘totally’, ‘only’.

Unique nouns rare in VQA and VQA-scene dataset. Another way to demonstrate the difference among 3DQA and VQA tasks is to show the top unique nouns that are rare in VQA and VQA-scene datasets. In Table 4 we present the analysis group by different scene types.

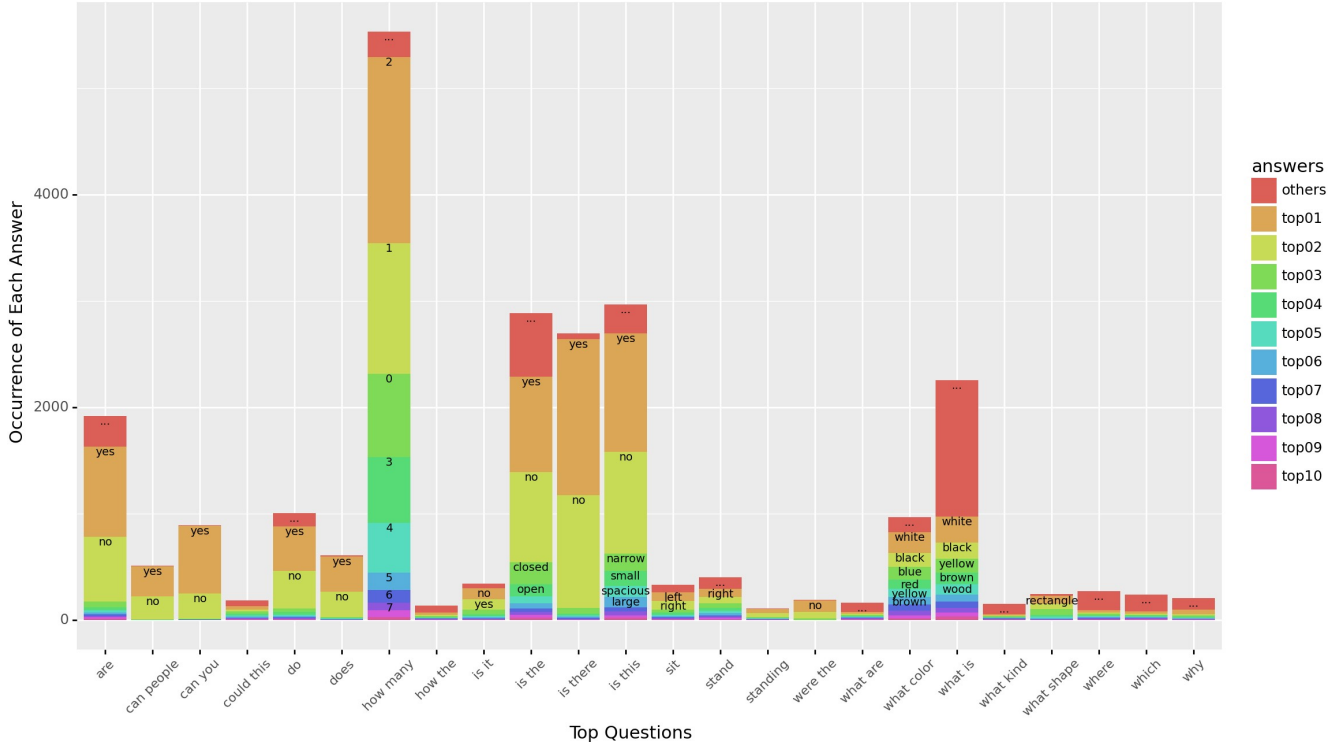


Figure 12. Answer occurrence distribution for each of the top question types in ScanQA.

Scenes	Nouns Rare in VQA & VQA-scene
Apartment	arrangement, instruments, doorway, bohemian
Bathroom	privacy, sanitation, towels, toilet, shower
Bedroom	asymmetrical, bedside, housekeeper, quilt
Classroom	whiteboard, chalkboard, projector, teacher
Conference	meeting, swivel, monitors, laptops
Laundry	ironing, washing, machines, dryers, washer
LivingRoom	spacious, industrial, scandinavian, neat

Table 4. Unique nouns rare in VQA and VQA-scene dataset.

10.2. Synthetic Dataset for Appearance Pretraining

To gain a better appearance feature representation before the final joint-training with the whole framework, we conduct a pretraining on a simple synthetically generated question answering dataset. This dataset is oriented for appearance information extraction – the question and answer pairs are only about colors of the objects. The templates for question generation are only two types ‘What color is the <ObjName>?’ (single object) or ‘What color are the <ObjName>?’ (multi objects), which is to avoid overfitting on language prior. In detail, to generate the questions, we utilize the annotated objects in ScanNet [13], except for the wall, floor, and ceiling classes. To generate the answers,

we first collect all points of the corresponding object with instance masks provided by ScanNet. And then, for each point, we find its color name by selecting its closest color among the seventeen named CSS 2.1 colors. Then, using all of the color names for each point in this object, we vote for one to two colors. For a single object, it is the final answer. For multi objects, we combine all the color names of individual objects to form the final answer.

10.3. Details on Human Accuracy Collection

In this section, we show the user interface and details for collecting human accuracy that are shown in Table 2 of our main paper. The left image in Fig. 13 shows the web-based

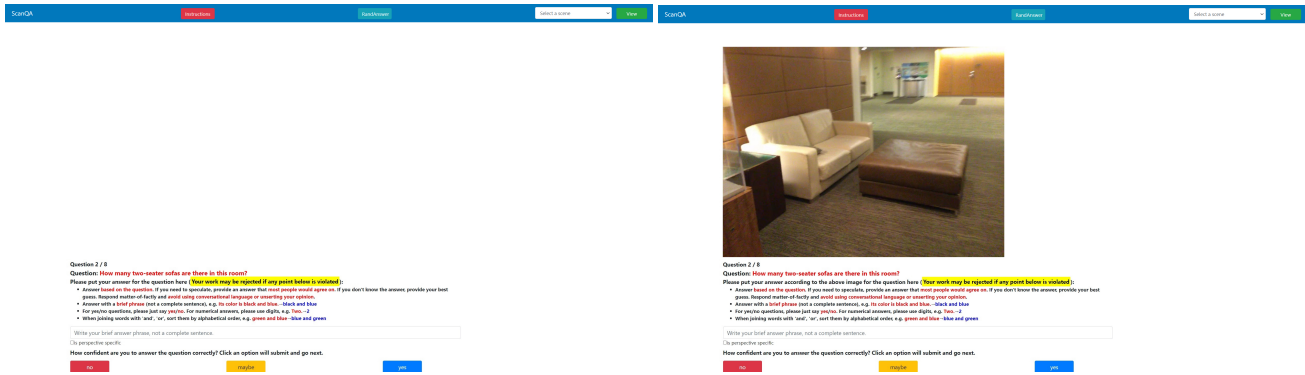


Figure 13. Our AMT interface for collecting the answer for input setting ‘Question’ and ‘Question+Image’ in our main paper.

Input	Human Accuracy (%)									
	All	Number	Color	Y/N	Other	aggregation	compare-avg	placement	spatial	viewpoint
Question+Caption	40.15	22.12	12.22	52.32	36.23	34.49	25.26	47.09	45.28	31.71
Question+Scene	73.89	82.42	47.03	89.16	56.59	76.45	75.00	71.28	77.08	70.02

Table 5. Accuracy of human answers given question and the captions in the corresponding scene.

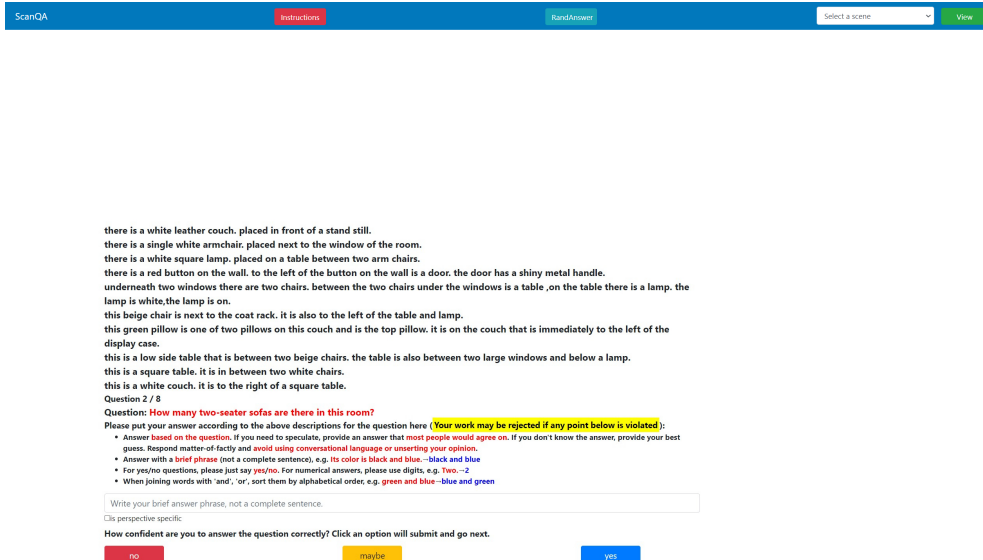


Figure 14. Our AMT interface for collecting the answer given captions but without showing frames or scenes.

UI for collecting human answers to input setting of ‘Question’ (to answer the question without frames or scenes). The right image shows the UI for the setting of ‘Question+Image’ (to answer the question with image frame). For the setting of ‘Question+Scene’, it shares the same UI with our answer collection. For fairness, the answers are collected by crowdsourcing on AMT, and the tested people are not the annotators for our ScanQA dataset.

We show an additional input setting in Fig. 14, where the tested people are given question and 10 referring expressions of different objects in this scene (Question+Caption). The captions are from ScanRefer [10]. The human accu-

racy in this setting is shown in Table 5. Notably, the accuracy is significantly lower than the people given scene, indicating that referring expressions are insufficient to solve 3DQA problems and emphasizing the importance of 3D scene comprehension in 3DQA.

10.4. Additional Implementation Details

The size of the candidate answer vocabulary is 166 for both training and testing. We train on 4 2080Ti GPUs with a total batch size of 64, using the AdamW optimizer [34] and an initial learning rate of $1.0e - 8$. The learning rate is updated according to the cyclical learning rate policy.

11. Additional Limitation

In addition to the limitation of scene variety as analyzed in our main paper, we encountered another shortcoming of our ScanQA dataset. As shown in Fig. 12, among the top questions, the answers for the questions that begin with ‘can you’ are heavily unbalanced - the proportion of ‘yes’ is roughly three times that of ‘no’ and other answers. Phenomenons like this in ScanQA exactly reflect the **real-world** data bias. However, this makes some questions generally answerable without requiring extensive scene comprehension. Despite carefully designed data collection methods for collecting interesting and diverse questions and high-quality answers, our task is still as likely to suffer from real-world prior, as a slew of widely used VQA datasets [4, 8, 19, 26, 30, 42, 47, 53, 57, 58] as studied in [2, 4, 22]. It may further affect the generalization ability of our framework.

For this issue, a number of efforts have been made in the past few years. Goyal et al. [22] and Zhang et al. [57] propose new datasets and data collection interfaces based on VQA to balance answer distribution. While the prior is controlled to some extent, the distribution in train and test set are still similar. Agrawal et al. [4] propose new splits of VQA to differ the question-answer distribution of train and test sets. Clevr [26] generates a diagnostic dataset with little biases to test the model’s visual reasoning abilities. GQA [25] extends it to real-world images by providing fine-grained scene graphs and developing an effective question generation method. Recently, we are witnessing more works on this issue [5, 11]. However, they are generally task-and-dataset specific, and it is non-trivial to apply on this 3DQA task. We are currently investigating data generation with extra annotations to perform systematical analysis and developing models with enhanced robustness to the bias. We believe our work, on the one hand, provides insights into the spatial aspects of the 3DQA task - 3D spatial understanding, navigation, and aggregation; on the other hand, it motivates future study on this challenging issue in this new field.